Alignment of Carbon Nanofibers in the Al$_2$O$_3$ Matrix under a Magnetic Field

Byung-Koog Jang[1,*], Kaoru Tsuda[2] and Yoshio Sakka[1]

[1]*Nano Ceramics Center, National Institute for Materials Science, Tsukuba 305-0047, Japan*
[2]*Nano Frontier Technology Co., Ltd., Tokyo 141-0032, Japan*

A stable suspension of multi-walled carbon nanofibers (CNFs) in Al$_2$O$_3$ was prepared by adding ammonium polycarboxylate as a dispersant in an aqueous solution. A strong magnetic field of 12 T was applied to the CNFs/Al$_2$O$_3$ suspension to investigate the alignment of the CNFs. The result was that the CNFs in the matrix showed good alignment with the direction of the magnetic field. It was found that 0.5 mass% CNFs showed isolated alignment; in contrast, with 5 mass% CNFs there were mainly aligned bundles. The alignment was only seen with straight CNFs; curved CNFs showed no alignment in a magnetic field. [doi:10.2320/matertrans.M2010326]

1. Introduction

Carbon nanoparticles, including carbon nanotubes (CNTs)[1] with dimensions from several to tens of nanometers and carbon nanofibres (CNFs)[2] with diameters of several hundreds of nanometers, have received enormous attention due to their superior properties in terms of electrical, physical, and mechanical behavior, and their applications in disciplines as diverse as biomedicine, optics, electronics, and structural engineering.

In particular, CNFs, due to their high tensile strength, modulus, excellent electrical, thermal properties and high aspect ratios have been widely studied as filler or reinforcing materials in advanced composites, such as polymers, epoxies, metals, ceramics, and nanocomposites.[2–8] Among the several types of CNFs, the new vapor-grown CNFs make mass production of fine quality carbon fibers possible at relatively low cost.[9,10]

In particular, the alignment of CNFs in the host matrix is one of the most interesting parameters in the fabrication of CNFs-dispersed composites.[11,12] Therefore, several studies on alignment using CNTs or CNFs have been reported, such as synthesis by CVD,[13–15] sputtering[16] and extrusion.[11] In addition, the reports have indicated that a strong magnetic field is very useful in producing the required textured structure, due to the alignment of particles in alloys[17] or ceramics.[18,19] Many materials have crystal magnetic anisotropy, in which the magnetic susceptibility differs along each crystal axis, and thus the crystals can be rotated to align in a preferred direction by the imposition of a strong magnetic field.[18–21]

We had already studied the influence of an applied strong magnetic field on the alignment of CNTs using CNT suspensions.[22] Therefore, the magnetic field method was the obvious choice for studying the alignment of CNFs with high aspect ratios. This had rarely been reported. In this work our investigation focused on the alignment behavior of CNFs in a green matrix of Al$_2$O$_3$, using a CNFs/Al$_2$O$_3$ suspension in a magnetic field.

Table 1 Properties of CNFs and Al$_2$O$_3$ powders.

Property	CNFs	Al$_2$O$_3$
Diameter (nm)	150	—
Length (µm)	10∼20	—
Aspect ratio	10∼500	—
Purity (%)	>99	>99.99
Surface area (m^2/g)	13	9∼15
Particle size (µm)		0.2

2. Experimental Procedure

We used commercial CNFs (Showa Denko Co., VGCF) fabricated by CVD, and Al$_2$O$_3$ powder (Sumitomo Chemical Co., AKP-50). The properties of pristine CNFs and Al$_2$O$_3$ powder are shown in Table 1. Ammonium polycarboxylate of 0.5 vol% was used as a dispersing agent, to improve the colloidal stability of the CNFs and alumina powder in the distilled aqueous solution by electrostatic repulsion.[15] First, alumina powder of 10 vol% solid content was poured into 200 ml of distilled water, and magnetically stirred. Next, 0.5∼5 mass% CNFs and the dispersing agent were slowly added to the alumina powder suspension, and again magnetically stirred, to obtain a CNFs/Al$_2$O$_3$ suspension. An ultrasound generator was placed in the beaker containing the CNFs/Al$_2$O$_3$ suspension, and the mixture was continuously stirred using a magnetic bar under ultrasonic agitation for 30 mins, to disperse and break up the bundles or agglomerates of CNFs.[23–25] Finally, a stable CNFs/Al$_2$O$_3$ suspension was obtained.

After that, 1 cc drops of the stable suspension were carefully dropped on a silicon wafer using a micropipette. The droplets of the CNF/Al$_2$O$_3$ suspension on the silicon wafers were carefully placed at the center of the magnetic field within the magnetic generator equipment. Then, a strong magnetic field of 12 T was applied to the specimens for 10 h, in order to investigate the alignment of the CNFs. After this period in the magnetic field, the specimens were dried at room temperature for 24 h.

The alignment and dispersed morphology of the CNF$_S$ in the alumina green matrix were determined by digital
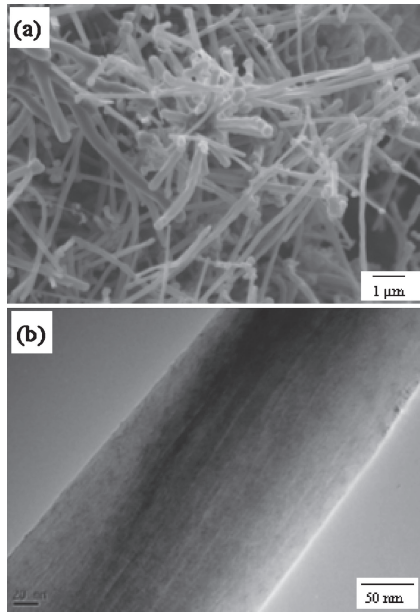
Fig. 1 Microstructure of multi-wall carbon nanofibers (CNFs): (a) SEM and (b) TEM.

Fig. 2 Digital micrographs of CNFs alignment for 0.5 mass% CNFs/Al$_2$O$_3$ sample in an applied magnetic field (the arrows indicate the direction of the magnetic field).

microscopy (Keyence, VHX-600), SEM (Jeol, JSM-6500), and TEM (Jeol, JEM-2100F). Phase analysis of the samples was performed using X-ray diffraction (XRD) (Jeol, JDX-3500) with Cu$K\alpha$ radiation. The particle size of the CNF$_S$ was evaluated by a laser particle analyzer (Otsuka Electronics). The zeta potential of the samples was measured, after being exposed to ultrasound for 10 mins, with a zeta potential analyzer (Otsuka Electronics, LSPZ-100 series).

3. Results and Discussion

Figure 1 shows typical micrographs of pristine CNFs. They are agglomerated/flocculated to form particle-like bundles because of the relatively strong van der Waals interactions between the fibres. The fibres appear to be relatively straight. The laser particle analyzer indicated average particle sizes of about 950 nm. The TEM micrograph of Fig. 1(b) indicates that their surfaces are clean, and show CNFs with 30~60 layers.

We successfully obtained a well-dispersed CNFs/alumina suspension. The zeta potential of this slurry was about -52 mV. Electrostatic repulsion between the relatively charged cluster surfaces plays a useful role in the stabilization of the CNF clusters in the solution, resulting in a stable suspension.

Figure 2 shows a low magnification digital micrograph of the aligned CNFs in a green alumina matrix in a magnetic field. The arrows indicate the direction of the magnetic field. There is clearly alignment of the CNFs along the magnetic field direction.

There was no concentration change of alumina and CNFs during drying at room temperature, because the CNFs/alumina suspension is non-volatile at room temperature. In addition, any influence of the drying procedure on the alignment of the CNFs can be ignored because the alignment is sustained throughout the drying period.
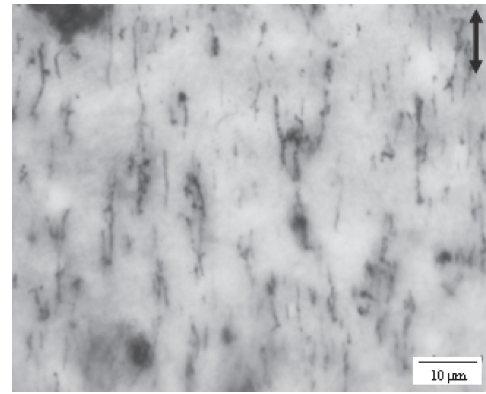
In general, the alignment mechanism of particles subject to a magnetic field can be explained as follows. When a strong magnetic field is applied to anisotropic ceramic particles in a stable suspension, the particles are rotated to an angle that minimizes the system energy by a magnetic torque resulting from the magnetic anisotropy of the particles.[18,19] Two conditions for alignment are then required: good dispersion and anisotropic magnetic susceptibility of the particles. The anisotropic energy transfer due to the anisotropic magnetic susceptibility is expressed by the following equation:[19]

$$\Delta E = -\Delta \chi V B^2/2\mu_0, \tag{1}$$

where $\Delta \chi = \chi_{a,b} - \chi_c$ is the anisotropy of the magnetic susceptibility, μ_0 is the permeability in vacuum, B is the applied magnetic field, and V is the volume of each particle. Alignment of anisotropic particles can occur when ΔE is greater than the thermal energy, $k_B T$.

For example, if the force along the c axis (the direction of the magnetic field) is greater than along the a or b axes, the particles show a well-textured structure, aligned in the c direction. CNFs generally have a high aspect ratio and an anisotropic structure. Consequently, CNFs can rotate in response to the magnetic field and align with the magnetic field direction, resulting in the aligned structure shown in Fig. 2.

We compared the effect of the magnetic field on CNF alignment in 0.5 mass% CNFs/Al$_2$O$_3$ sample and 5 mass% CNFs/Al$_2$O$_3$ sample, as shown in the SEM results of Fig. 3. With no magnetic field, CNFs were seen randomly dispersed in the Al$_2$O$_3$ matrix, as shown in Figs. 3(a) and (c). In contrast, in an applied magnetic field, the CNFs of both samples were seen to be aligned in the vertical direction, corresponding to the direction of the magnetic field, as shown in Fig. 3(b) and (d). The arrows in Fig. 3 indicate the direction of the magnetic field.

The SEM results show only isolated alignment of the CNFs in Fig. 3(b). In comparison, Fig. 3(d) shows mainly aligned bundles, suggesting that the alignment of CNFs depends on their concentration.

Some CNFs were not aligned perfectly parallel to the direction of magnetic field. This can be explained as follows. CNFs were initially randomly dispersed, as shown in
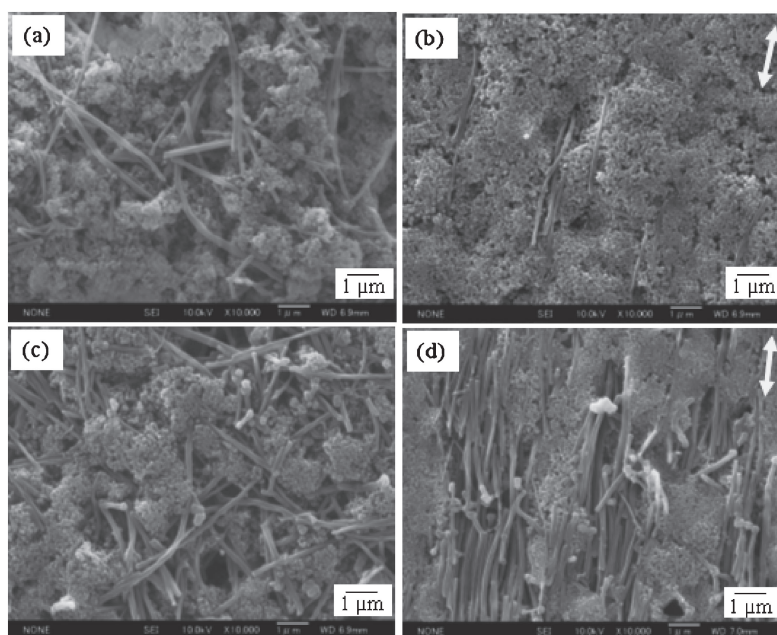
Fig. 3 SEM micrographs of the effect of a magnetic field on CNFs alignment for 0.5 mass% CNFs/Al$_2$O$_3$ sample (upper, (a) and (b)) and 5 mass% CNFs/Al$_2$O$_3$ sample (lower, (c) and (d)): (a) and (c) without a magnetic field; (b) and (d) with a magnetic field (the arrow indicates the direction of the magnetic field).
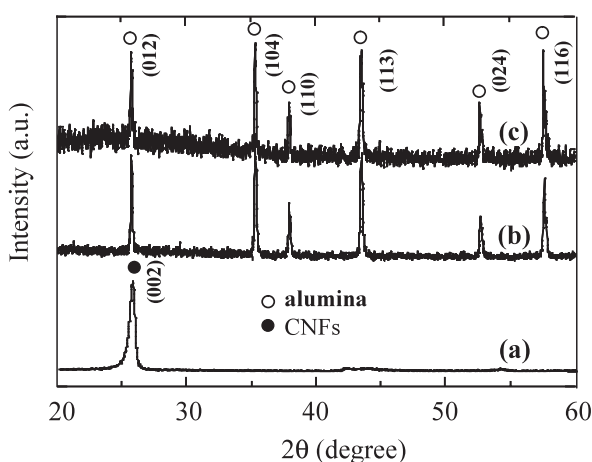

Fig. 4 XRD results of (a) pristine CNFs, (b) 0.5 mass% CNFs/Al$_2$O$_3$ sample without a magnetic field, and (c) 0.5 mass% CNFs/Al$_2$O$_3$ sample with a magnetic field.

Fig. 5 SEM micrograph of curved CNFs for 0.5 mass% CNFs/Al$_2$O$_3$ sample under a magnetic field (both arrows indicate the direction of the magnetic field).

Fig. 3(a) and (c). CNFs suspended in an aqueous solution without any matrix could rotate freely to line up parallel to the magnetic field. When the magnetic field was applied to the CNFs/alumina suspension, however, the alumina matrix may have impeded the free rotation of some CNFs. The tendency of neighboring CNFs to rotate resulted in the bundles shown in Fig. 3(d) for a higher concentration of CNFs.

Figure 4 shows the XRD results of the CNFs/Al$_2$O$_3$ samples with and without the magnetic field. The main peak of pristine CNFs in Fig. 4(a) appears at about 26° and corresponds to the (002) layers of the graphite structure.[26] The main peak of CNFs in the CNFs/Al$_2$O$_3$ samples overlaps with the (012) peak of alumina, as shown in Fig. 4(b) and (c). The XRD patterns of Al$_2$O$_3$, both without magnetic field (Fig. 4(b)) and with magnetic field (Fig. 4(c)), are the same, and their peaks show the α-alumina phase. This means that there has been no crystallographic re-orientation of the Al$_2$O$_3$ matrix in the presence of the magnetic field. The crystallographic orientation of Al$_2$O$_3$ particles may be disturbed due to the existence of CNFs in the samples. Contrary to these results, alumina sintered at 1873 K has shown crystallographic re-orientation in a magnetic field[18] and the XRD results closely depend on the surface position (parallel, vertical) of sintered Al$_2$O$_3$ samples relative to the magnetic field direction. This implies that the crystallographic structure of sintered alumina[18] is generally better, due to the preferred crystallographic orientation, than the green alumina matrix used in the present work.

A further result was that curved CNFs, indicated by an arrow in Fig. 5, exhibited no alignment in a magnetic field, even though most CNFs were aligned with the field direction.

This indicates that the degree of alignment of CNFs depends on their shape. Consequently, straight CNFs can be considered better for alignment than curved ones, as has been previously found in studies of CNT alignment.[22]

The outcome of this work suggests that the application of a magnetic field is very effective for aligning CNFs. This aligning ability of CNFs is expected to lead to the development of nanocomposites with desirable structural and functional properties, and further study is being carried out to verify this.

4. Conclusions

The influence of a magnetic field on the alignment of CNFs in an Al₂O₃ green matrix was studied. Good dispersal of CNFs in the Al₂O₃ matrix was achieved using ammonium polycarboxylate as a dispersant in a distilled aqueous solution. Well-aligned CNFs in the matrix were successfully obtained with a strong magnetic field of 12 T. The degree of alignment of the CNFs with the magnetic field depended on the shape of CNFs. Curved CNFs were shown not to align in a magnetic field. Straight CNFs are therefore better than curved ones where alignment is required. These results suggest that it is possible to develop CNFs-dispersed composites with an aligned percolation structure of CNFs.

Acknowledgments

REFERENCES

1) S. Iijima: Nature **354** (1991) 56–58.
2) M. Endo, Y. A. Kim, T. Hayashi, K. Nishimura, T. Matushita, K. Miyashita and M. S. Dresselhaus: Carbon **39** (2001) 1287–1297.
3) J. F. Silvain, C. Vincent, J. M. Heintz and N. Chandra: Compos. Sci. Technol. **69** (2009) 2474–2484.
4) K. Hirota, H. Hara and M. Kato: Mater. Sci. Eng. A **458** (2007) 216–225.
5) Y. Zhou, F. Pervin, V. K. Rangari and S. Jeelani: Mater. Sci. Eng. A **426** (2006) 221–228.
6) H. A. Mohammed and U. Sundararaj: Carbon **47** (2009) 2–22.
7) G. G. Tibbetts, M. L. Lake, K. L. Strong and B. P. Rice: Compos. Sci. Technol. **67** (2007) 1709-18.
8) A. Duszova, J. Dusza, K. Tomasek, J. Morgiel, G. Blugand and J. Kuebler: Scr. Mater. **58** (2008) 520–523.
9) T. Koyama: Carbon **10** (1972) 757–758.
10) Y. K. Choi, K. Sugimoto, S. M. Song and M. Endo: Mater. Lett. **59** (2005) 3514–3520.
11) M. M. Hasan, Y. Zhou and S. Jeelani: Mater. Lett. **61** (2007) 1134–1136.
12) K. Satish, H. Doshi, M. Srinivasarao, J. O. Park and D. A. Schiraldi: Polymer **43** (2002) 1701–1703.
13) Z. F. Ren, Z. P. Huang, J. W. Xu, J. H. Wang, P. Bush, M. P. Siegal and P. N. Provencio: Science **282** (1998) 1105–1107.
14) C. Bower, W. Zhu, S. Jin and O. Zhou: Appl. Phys. Lett. **77** (2000) 830–832.
15) L. Valentinia, I. Armentanoa, J. M. Kennya, L. Lozzib and S. Santucci: Mater. Lett. **57** (2003) 3699–3704.
16) N. Hayashi, S. Honda, K. Tsuji, K. Lee, T. Ikuno, K. Fujimoto, S. Ohkura, M. Katayama, K. Oura and T. Hirao: Appl. Surf. Sci. **212–213** (2003) 393–396.
17) Y. Han, C. Ban, S. Guo, X. Liu, Q. Ba and J. Cui: Mater. Lett. **61** (2007) 983–986.
18) T. S. Suzuki, T. Uchikoshi and Y. Sakka: J. Ceram. Soc. Jpn. **114** (2006) 59–62.
19) Y. Sakka and T. S. Suzuki: J. Ceram. Soc. Jpn. **113** (2005) 26–36.
20) S. Asai, K. Sassa and M. Tahashi: Sci. Technol. Adv. Mater. **4** (2003) 455–460.
21) P. Rango, M. Lees, P. Lejay, A. Sulpice, R. Tournier, M. Ingold, P. Germi and M. Pernet: Nature **349** (1991) 770–771.
22) B. K. Jang and Y. Sakka: Mater. Lett. **63** (2009) 2545–2547.
23) B. K. Jang and Y. Sakka: Mater. Trans. **51** (2010) 192–195.
24) M. Sano, A. Kamino, J. Okamura and S. Shinkai: Science **293** (2001) 1299–1301.
25) J. M. Bonard, T. Stora, J. P. Salvetat, F. Maier, T. Stöckli, C. Duschl, L. Forró, W. A. Heer and A. Châtelain: Adv. Mater. **9** (1997) 827–831.
26) V. S. Babu and M. S. Seehra: Carbon **34** (1996) 1259–1265.